A Study of the Structure of the Lyomesophases Formed by the Dinucleoside Phosphate d(GpG). An Approach by X-ray Diffraction and Optical Microscopy

Paolo Mariani,*,† Claude Mazabard,† Anna Garbesi,‡ and Gian Piero Spada*,§

Contribution from the Istituto di Fisica Medica, Università di Ancona, Monte d'Ago, I-60131 Ancona, Italy, I.Co.C.E.A.-CNR, via della Chimica 8, I-40064 Ozzano Emilia, Italy, and Dipartimento di Chimica Organica, Università di Bologna, via S. Donato 15, I-40127 Bologna, Italy. *Received December 22, 1988*

Abstract: The sodium salt of the dinucleoside phosphate d(GpG) in aqueous solution forms cholesteric and hexagonal mesophases. We suggest that these liquid crystalline phases consist of rod-shaped aggregates with negative diamagnetic anisotropy. Each rod is composed by a stacked array of planar tetramers formed by Hoogsteen-bonded guanosine moieties. Optical microscopy and X-ray diffraction support this model.

In a recent note[1] some of us reported that the aqueous solution of 2′-deoxyguanylyl-(3′→5′)-2′-deoxyguanosine (d(GpG)) sodium salt may exhibit liquid crystalline phases.

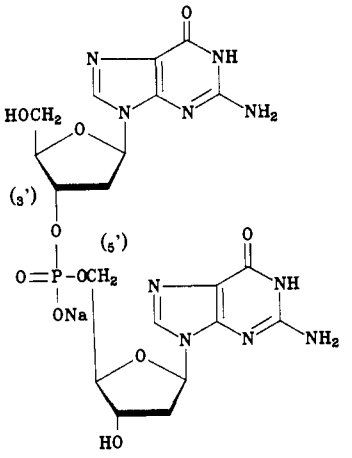

The peculiar ability of "sticky" guanosine and some of its derivatives to self-associate into stable structures[2-4] has been known for a long time; highly ordered gels, fibers, and other macroaggregates have been investigated. The common basic building block of such structures is a planar unit formed by four guanines, hydrogen bonded in a "Hoogsteen mode".[3-5]

The interest in this special feature of guanosine has been greatly renewed by the very recent report[6] that "single-stranded DNA, containing short guanine-rich motifs, self-associate at physiological salt concentration to make four-stranded structures in which the strands run in parallel fashion". The authors suggest that the self-recognition of guanine-rich regions serves to bring together the four homologous chromatids during meiosis.

It had already been suggested that self-ordering of guanosine derivatives could have had prebiotic significance: 5′-guanylic acid aggregates discriminate between glycine and alanine,[7] two of the most abundant archaic amino acids, and this fact may have had a role in the origin of the genetic code; these self-ordered aggregates could have acted as a template of the first polynucleotide; guanosine tetrameric aggregates are potential ionophores for K^+ and Na^+ ions.[8] Though some of these hypotheses may be mere speculations, "biological activity demands organization. Aggregation provides one level of organization of molecules and it is reversible."[9]

In the light of the above reported evidences it seemed worthwhile to get a better insight into the nature and geometry of the interactions of guanosine derivatives aggregates.

In the present paper we report on the structure of the lyomesophases of d(GpG) by means of optical microscopy and X-ray diffraction. The former technique gives information especially about the cholesteric phase, while by X-ray diffraction direct structural information was obtained on both cholesteric and hexagonal phases.

Experimental Section

Synthesis of 2′-Deoxyguanylyl-(3′→5′)-2′-deoxyguanosine [d(GpG)]. The dinucleoside monophosphate was prepared according to a known procedure[10] and purified by column chromatography (LiChropsep RP-18, eluent: linear gradient from 0 to 15% of CH_3CN in 0.05 M TEAB, pH 7.5). Following HPLC analysis (Spherisorb SiO ODSi, eluent: gradient from 0 to 12% of CH_3CN in 0.05 M KH_2PO_4, pH 4.5, column temperature 38 °C), the fractions with purity ≥95% were pooled and, after repeated coevaporations with water, treated with Dowex 50WX8 (Na^+ form). The final product, after repeated coevaporation with absolute ethanol, was analyzed by TLC, HPLC, and UV spectroscopy. The residual molar extinction at the absorption maximum (λ = 252 nm, solvent: water) is 1.06×10^4 M^{-1} cm^{-1}. The spectra of a solution of 10^{-4} M were recorded at room temperature, 80 °C, and again at room temperature after cooling; the variation of the extinction was within 1%.

X-ray Diffraction. X-ray diffraction experiments have been performed by using a conventional X-ray generator equipped with a temperature-controlled Guiner camera, operating in vacuo: the X-ray beam was monochromatized and focused by a bent quartz crystal, which isolates the Cu $K\alpha_1$ line. Some experiments were also performed with a rotating anode generator Rigaku Denki RV 300 equipped with a powder diffractometer: Ni-filtered Cu $K\alpha$ radiation (λ = 1.54 Å) was used. In all cases the samples, prepared at specific concentrations and left at least for 1 day at room temperature to avoid dishomogeneous mixtures, were held in a vacuum-tight cylindrical cell, provided with two thin mica windows. The temperature was controlled with an accuracy of ±0.5 °C

† Università di Ancona.
‡ ICoCEA-CNR.
§ Università di Bologna.

(1) Spada, G. P.; Carcuro, A.; Colonna, F. P.; Garbesi, A.; Gottarelli, G. *Liq. Cryst.* **1988**, *3*, 651-4.
(2) Saenger, W. *Principles of Nucleic Acid Structure*; Springer-Verlag: New York, 1984; pp 315-20.
(3) Gellert, M.; Lippsett, M. N.; Davis, D. R. *Proc. Natl. Acad. Sci. U.S.A.* **1962**, *48*, 2013. Chantot, J. F.; Sarocchi, M. T.; Gushlbauer, W. *Biochemie* **1971**, *53*, 347. Tougard, P.; Chantot, J. F.; Gushlbauer, W. *Biophys. Biochem. Acta* **1973**, *308*, 9-16. Chantot, J. F.; Haertle, T.; Gushlbauer, W. *Biochemie* **1974**, *56*, 501. Zimmermann, S. B. *J. Mol. Biol.* **1976**, *106*, 663-72.
(4) Pinnavaia, T. J.; Miles, H. T.; Becker, E. D. *J. Am. Chem. Soc.* **1975**, *97*, 7198-200. Borzo, M.; Detellier, C.; Laszlo, P.; Paris, A. *J. Am. Chem. Soc.* **1980**, *102*, 1124-34.
(5) Hoogsteen, K. *Acta Crystallogr.* **1959**, *12*, 822-3.
(6) Sen, D.; Gilbert, W. *Nature (London)* **1988**, *334*, 364-6.
(7) Detellier, C.; Laszlo, P. *Helv. Chim. Acta* **1979**, *62*, 1559-65.
(8) Pinnavaia, T. J.; Marshall, C. L.; Mettler, C. M.; Fisk, C. L.; Miles, H. T.; Becker, E. D. *J. Am. Chem. Soc.* **1978**, *100*, 3625-7. Detellier, C.; Laszlo, P. *J. Am. Chem. Soc.* **1980**, *102*, 1135-41.
(9) Florence, A. G. In *Micellisation, Solubilisation, and Microemulsions*; Mittal, K. L., Ed.; Plenum Press: New York, 1977; Vol. 1, pp 55-74.
(10) Marugg, J. E.; Tromp, M.; Jhurani, P.; Hoyng, C. F.; van der Marel, G. A.; van Boom, J. H. *Tetrahedron* **1985**, *40*, 73-8.

0002-7863/89/1511-6369$01.50/0

Table I. Unit Cell Dimension (a) and Concentration (c) of Some Samples in the Hexagonal Phase[a]

	c = 20%; a = 63.7 Å			c = 30%; a = 53.7 Å			c = 38%; a = 47.2 Å			c = 50%; a = 37.2 Å		
$(h^2 + k^2 - hk)^{1/2}$	S_{obs}	S_{clc}	I_{obs}	S_{obs}	S_{clc}	I_{obs}	S_{obs}	S_{clc}	I_{obs}	S_{obs}	S_{clc}	I_{obs}
$\sqrt{1}$	18.1	18.1	8608	21.5	21.5	8791	24.4	24.5	9318	31.1	31.1	9640
$\sqrt{3}$	31.5	31.4	452	37.3	37.2	470	42.3	42.3	373	53.9	53.8	237
$\sqrt{4}$	–	36.2	0	42.7	43.0	293	49.0	48.9	309	61.7	62.1	123
$\sqrt{7}$	48.0	47.9	940	57.0	56.9	446	–	64.7	0	–	82.2	0
$\sqrt{9}$	–	54.3	0	–	64.5	0	–	73.4	0	–	93.2	0

[a] S_{obs} is the reciprocal spacing (expressed in 10^{-3} Å^{-1}) of the observed reflection, while S_{clc} is the calculated one for a bidimensional hexagonal structure with the reported lattice parameter a. I_{obs} is the observed intensity calculated as reported in ref 19 and normalized to $\sum I_{obs}$ = 10000.

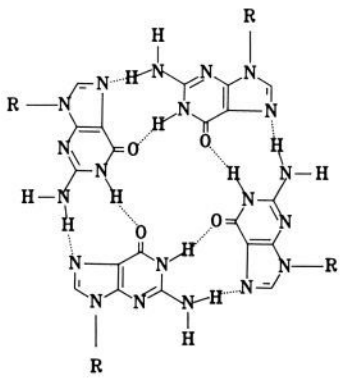

Figure 1. Tetrameric arrangement of guanine bases bonded in a Hoogsteen mode.

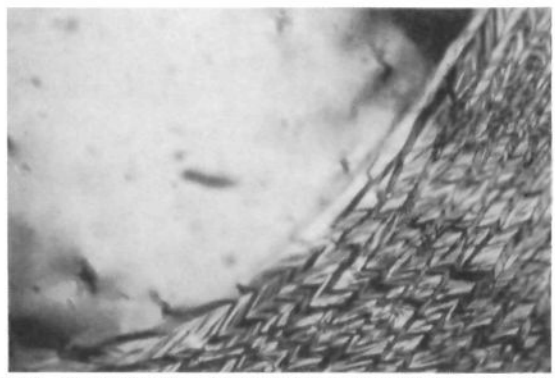

Figure 2. Textures obtained by peripheral evaporation of a cholesteric solution of d(GpG). The picture shows the transition between the cholesteric (upper left side) and the hexagonal (lower right side) phases (crossed polars, magnification 250×).

by using a circulation thermostat. The electron density of water was assumed to be 0.33 e$^-$ Å^{-3}, while that of d(GpG) was 0.47 e$^-$ Å^{-3}.

Optical Microscopy. Microscopic observations were performed with a Zeiss polarizing microscope equipped with a photocamera. Preliminary observations were done on peripheral evaporation samples. Cholesteric solutions were inserted into rectangular capillaries (thickness 0.3 mm) sealed with epoxy resin; the samples were then oriented putting them in a 5 kG magnet for ca. 5 h, and the textures were observed between crossed polars. Hexagonal samples were examined instead in a glass slide with or without coverslip.

Results

We have studied the binary system formed by the sodium salt of d(GpG) and water at different concentrations and temperatures. The phase sequence at constant temperature (20 °C) as a function of the concentration of d(GpG) is

$$\mathrm{I} \xrightarrow{2.5\%} \mathrm{N^*} \xrightarrow{18\%} \mathrm{H} \xrightarrow{\sim 65\%} \mathrm{K}$$

where I, N*, H, and K denote isotropic, cholesteric, hexagonal, and crystal phases, respectively. In the present paper concentration is expressed as weight of d(GpG) over the total weight.

Optical Microscopy. Previous microscopy observations of samples with concentration gradient obtained by peripheral evaporation[1] have shown the existence of at least two different liquid crystalline phases, which were identified as cholesteric (N*) and hexagonal (H) at higher and lower water content, respectively. The very dilute solution (concentration below 2.5%) appears to be colorless, transparent, and fluid and does not show birefringence: this phase corresponds to the isotropic solution.

When the d(GpG) concentration is in the range between 2.5 and 18%, the phase exhibits a typical cholesteric texture.[1] It is possible to align the cholesteric axis applying a magnetic field perpendicular or parallel to the cell walls to obtain planar or fingerprint textures, respectively[11] (see Figure 3). This behavior and the absence of unwinding by the field is in agreement with a cholesteric formed by structural units with negative diamagnetic anisotropy (type II cholesteric).[12]

The helix pitch decreases with increasing concentration,[1] a behavior which parallels that of polypeptide cholesterics.[13] For cellulose derivatives, instead, the opposite trend is observed.[14]

In the region between 20 and 60%, the texture shows herring-bone patterns,[1] similar to those reported for the hexagonal columnar phases formed by disodium chromoglycate,[15] other chromonics,[16] and DNA:[17] this phase was thus identified as hexagonal.[1]

At lower water content, the texture does not show any observable modification: it shows birefringence, and no phase transitions appear to take place. It must be noticed that phase transitions were not observed by increasing or decreasing the temperature in the range 5–50 °C.

X-ray Diffraction. Two typical diffraction patterns obtained from mixtures containing 10 and 50% of d(GpG) are shown in Figure 4. Only a very broad and weak peak is observed in the small angle region in the case of a 10% sample, as it would be expected for a cholesteric (or nematic) liquid crystalline phase. The high angle region appears to be characterized by the presence of a broad band, which is due to the excess of water, and by a superposed sharp peak corresponding to a spacing of 3.3 Å.

When the content of water is decreased, the diffraction pattern changes and becomes more structured. From d(GpG) concentration greater than 20% the X-ray small angle diffraction pattern consists of a very strong peak, coupled with few very weak peaks (see Figure 4); the ratios of their spacings in unit S[18] are $1{:}\sqrt{3}{:}\sqrt{4}{:}\sqrt{7}$..., and they can therefore be indexed unambiguously in terms of a two-dimensional hexagonal lattice. In the high

(11) Radley, K.; Saupe, A. *Mol. Phys.* **1978**, *42*, 493. Yu, L. J.; Saupe, A. *J. Am. Chem. Soc.* **1980**, *102*, 4879.

(12) Boden, N.; Radley, K.; Holmes, M. C. *Mol. Phys.* **1981**, *42*, 493. Alcantara, M. R.; De Melo, M. V. M. C.; Paoli, V. R.; Vanin, J. A. *Mol. Cryst. Liq. Cryst.* **1983**, *95*, 299. Melnik, J.; Saupe, A. *Mol. Cryst. Liq. Cryst.* **1987**, *145*, 95–110.

(13) Robinson, C. *Tetrahedron* **1961**, *13*, 219–34. Rao, M. V. R.; Atreyi, M.; Pantar, A. V. *Liq. Cryst.* **1987**, *2*, 889–93.

(14) Steinmeier, H.; Zugenmeier, P. *Carbohydr. Res.* **1988**, *173*, 75–88.

(15) Hartshorne, N. H.; Woodard, G. D. *Mol. Cryst. Liq. Cryst.* **1973**, *23*, 343–68.

(16) Attwood, T. K.; Lydon, J. E. *Mol. Cryst. Liq. Cryst.* **1984**, *108*, 349–57.

(17) Livolant, F.; Bouligand, Y. *J. Physique* **1986**, *47*, 1813–27.

(18) $S_{hk} = 2 \sin \theta/\lambda$, where 2θ is the scattering angle, λ the X-ray wavelength, and h,k the Miller indices of the reflection. By using the convention usually adopted in lipid crystallography,[19,20] the symmetry-permitted reflections in the case of the bidimensional hexagonal phase are given by $S = (1/a)\cdot(h^2 + k^2 - hk)^{1/2})$, where a is the unit cell dimension.

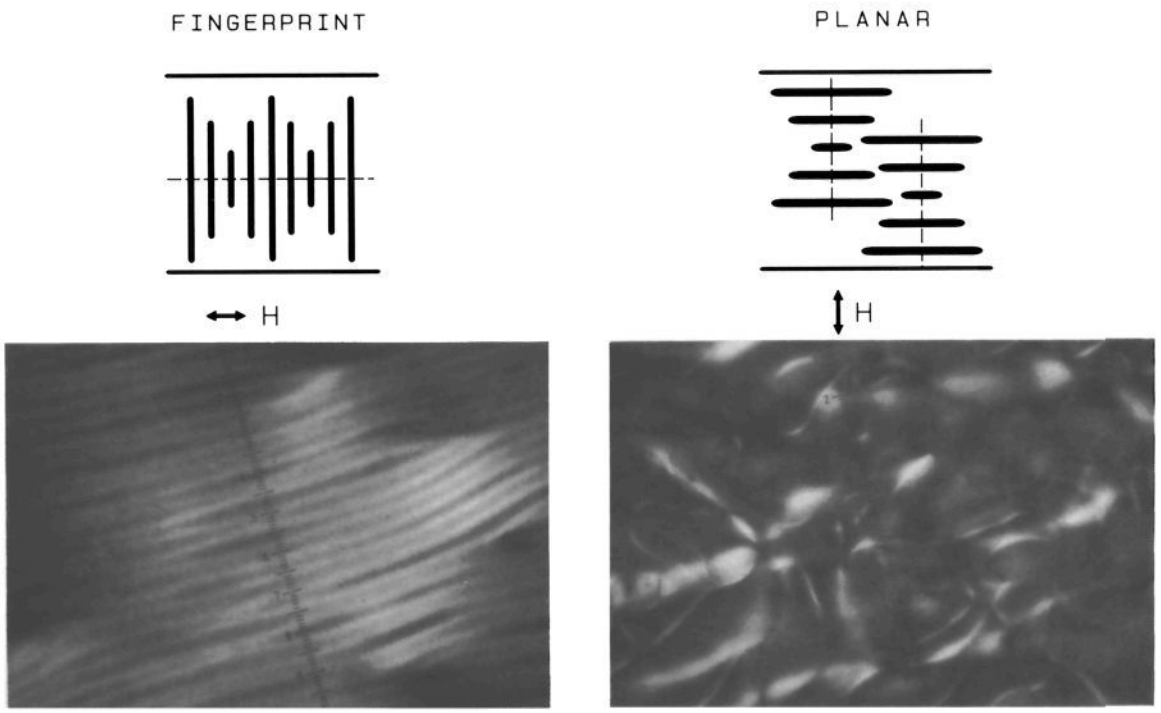

Figure 3. The two limiting orientation modes ("fingerprint" and "planar") and their microscopic textures of a cholesteric whose building blocks possess a negative diamagnetic anisotropy. The bars represent the symmetry axes of the aggregates, and the double arrows indicate the direction of application of the magnetic field H. The photographs were taken with crossed polars; the unit scale is 40 Å.

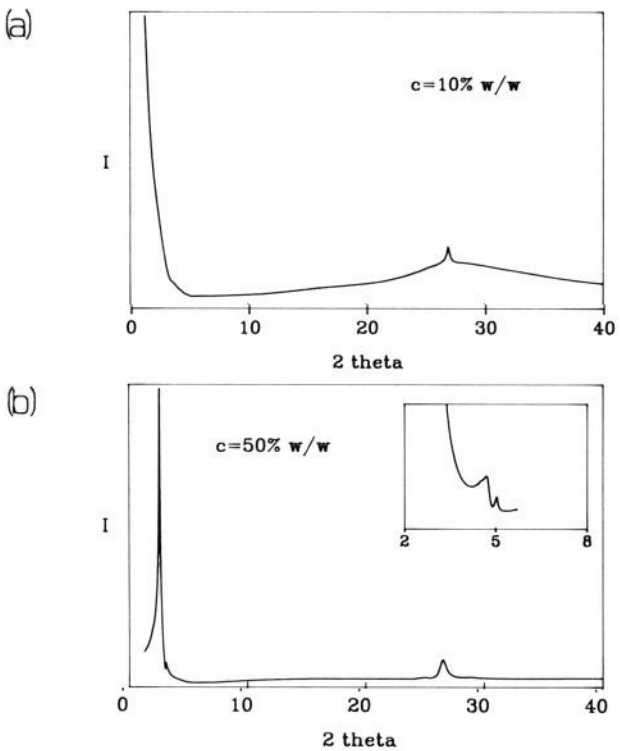

Figure 4. X-ray diffraction diagrams of a cholesteric (a, c = 10%) phase and of a hexagonal (b, c = 50%) one at 20 °C.

angle region, the sharp peak corresponding to a spacing of 3.3 Å still remains. Table I reports, for some of the investigated samples in the hexagonal phase, the low angle X-ray diffracted peak position together with the observed intensities.

The spacing of the reflections appears to be a function of concentration; Figure 5 presents the unit cell dimension, calculated by using $a = 2/(S\sqrt{3})$, as a function of the concentration. It is also interesting to notice that the lattice constant and the peak

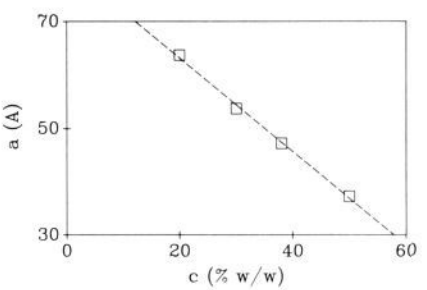

Figure 5. Variation of the hexagonal lattice parameter a (calculated at 20 °C from the spacings of the X-ray diffraction peaks) as a function of d(GpG) concentration.

Table II. The Radius of the Cylinder (R_{rod})[a]

c (%)	20	30	38	50
c_v	0.141	0.219	0.285	0.395
a (Å)	63.7	53.7	47.2	37.2
R_{rod} (Å)	12.6	13.2	13.2	12.3

[a] Calculated by supposing a straight rod of circular section containing only d(GpG) molecules (eq 1, see text). c_v is the volume concentration (calculated by using the value of 0.651 cm^3 g^{-1} as specific volume),[21] and a is the unit cell dimension.

intensities do not show any detectable dependence from the temperature in the range 5–50 °C.

For d(GpG) concentration larger than about 60%, the diffraction profile exhibits sharper reflections superimposed to the hexagonal ones. This pattern indicates a more highly ordered phase and is quite similar to that observed in the d(GpG) crystals. Since the relative intensity of the peaks due to the hexagonal order appears to decrease when the water content decreases, a large biphasic region precedes the appearance of the pure crystalline phase.

Our attention was focused on the hexagonal phase. By using the method described by Luzzati[20] in analogy with classical

(19) Tardieu, A. Thesis, Université Paris-Sud, 1972. Luzzati, V.; Gulik-Krzywicki, T.; Tardieu, A. *Nature* (*London*) **1968**, *218*, 1031–4.

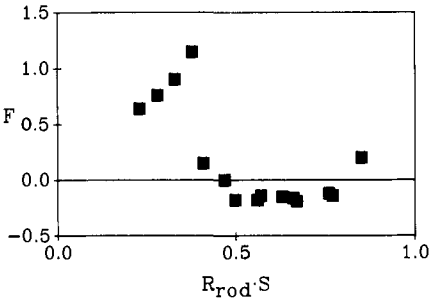

Figure 6. Determination of the signs of the structure factors in the hexagonal phase. The experiments were performed at 20 °C and at different water content. The structure factors are plotted as a function of the R_{rod}·S product.

hexagonal phases, and then by assuming a model with d(GpG) rod-like aggregates in a continuum of water, with the polar phosphate groups on the outside of the cylinders, and assuming, as usual, that water does not penetrate the rods (in the present case such assumption seems to be realistic; see ref 3), we have determined the rod dimension.

Table II reports the rod radius calculated by eq 1

$$R_{rod} = (\sigma c_v/2\pi)^{1/2} \quad (1)$$

where σ is the unit cell surface, and c_v is the volume concentration of d(GpG). It must be noticed that the radius remains almost constant, ca. 13 Å, when the water content in the sample changes. This finding perfectly agrees with the assumption that the cylinders contain just d(GpG) molecules and are embedded in the water matrix.

From the small angle diffraction pattern ($S < (10\ Å)^{-1}$) we have calculated the electronic density profile of a hexagonal phase. In fact from the observed diffracted peak intensities, it is possible to obtain the structure factors and then, if their signs are known, the electron density distribution. In this case the "phase problem", i.e., the correct assignment of the sign of the structure factors, has been solved as follows. It is possible to assume, at a first approximation, that at all concentrations the electron density distribution inside the cylinders is a radial function of the ratio R/R_{rod} and that the electron density is fairly uniform outside the rods. In this case we expect that at all concentrations the structure factors will sample a continuous function of the product R_{rod}·S. Then, by using "swelling" experiments, it is possible to determine the phase angles of the reflections. Figure 6 reports the structure factors of different observed small angle reflections plotted as a function of the product R_{rod}·S: the positions of sign inversions are easily identified.

Finally, by using the correct assignment of the signs and after data normalization[22] which leads to dimensionless expressions of both the structure factors and the electron density distribution, we have obtained the electron density maps. As an example, Figure 7 reports the structure of the hexagonal phase of the sample containing 50% of d(GpG): the map clearly shows the electron dense rod section, which after our normalization appears to be positive, while the outside rod region is sufficiently smooth to indicate the water and is negative owing to the lower value of the water electron density with respect to d(GpG) molecule. As usual in crystallographic analyses, the most convincing argument in support of the proposed structure is the agreement of the electron density map with the data obtained from chemical composition (see, e.g., eq 1) not involved in the structure analysis. In our case the dimension of the cylindrical elements, which can be directly obtained from the zero density level in the map, is in excellent agreement with the experimental data reported in Table II, and this supports strongly the proposed structure.[23]

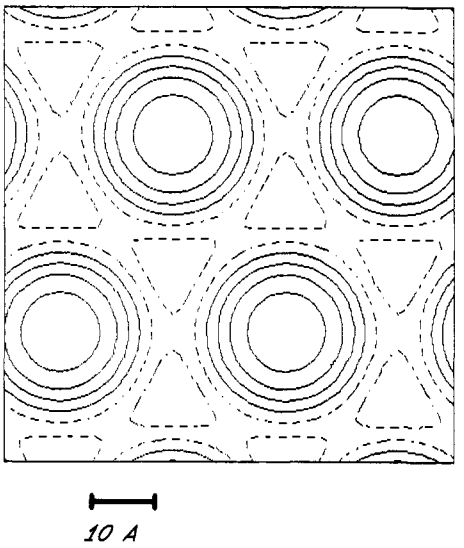

Figure 7. Electron density distribution of the hexagonal phase in the 50% sample; the scale of electron density is arbitrary (see ref 22 for the data normalization), and the density line is equally spaced with negative values dotted. The sign combination of the structure factors (see Table I and Figure 6) is +−−00.

Discussion

Classical lyotropic liquid crystalline phases are formed by amphiphilic compounds, such as lipids and detergents dissolved in water with or without cosurfactants and electrolytes.[24] Above a critical concentration (cmc), molecules aggregate into micelles. Micelles are spherical in shape just above cmc; by increasing amphiphile concentration they became anisometric (disk-like or cylindrical), and their interactions may stabilize a nematic phase.[25] At still higher concentrations, a discotic nematic usually evolves to a lamellar phase, while a cylindrical nematic evolves to a hexagonal phase (i.e., a hexagonal array of cylindrical micelles).[24] With chiral amphiphiles or in the presence of chiral dopants, a cholesteric phase is formed instead of the nematic one.

More recently, molecules whose structure differs from that of a classical amphiphile have been shown to exhibit a lyotropic mesomorphism. Examples are disodium chromoglycate[15,26] and related antiasthmatic drugs,[16] water soluble dyes,[27] and discoid molecules.[28] All these compounds are characterized by the presence of polar groups distributed throughout an aromatic core

(20) Luzzati, V. In *Biological Membranes*, Chapman, D., Ed.; Academic Press: London, 1968; Chapter 3.
(21) Iball, J.; Morgan, C. H.; Wilson, H. R. *Nature (London)* **1963**, *199*, 688–9.
(22) Mariani, P.; Luzzati, V.; Delacroix, H. *J. Mol. Biol.* **1988**, *204*, 169–89.

(23) Alternatively we can determine the sign of F_{obs} introducing a proper function in f_s. In fact the intensity I_{hk} of each diffraction peak verifies the following equation[19]

$$I_{hk} = m \cdot F_{obs}^2 = m \cdot f_s^2$$

where m is the multiplicity and f_s the form factor. Since the form factor of a uniform cylinder of radius R_{rod} is

$$f_s = J_1(2\pi R_{rod} \cdot S)/\pi R_{rod} \cdot S$$

where J_1 is the Bessel function one, the position of zeros (sign inversions) at $2\pi R_{rod}S' = 3.83$ and $2\pi R_{rod}S'' = 7.02$ are

$$R_{rod}S' = 0.61 \qquad R_{rod}S'' = 1.12$$

By considering the observed structure factors reported in Figure 6, it can be noticed that the agreement with the observed values cannot be considered satisfactory, indicating that a J_1 model does poorly in representing the true form factor of rods (see the electron density profile inside the rods in the map in Figure 7).

(24) Forrest, B. J.; Reeves, L. W. *Chem. Rev.* **1981**, *81*, 1.
(25) Saupe, A. *Nuovo Cimento* **1984**, *3*, 16. Hendrikx, Y.; Charvolin, J. *J. Physique* **1982**, *42*, 1427. Kuzma, M. R. *J. Phys. Chem.* **1985**, *89*, 4124.
(26) Goldfarb, D.; Luz, Z.; Spielberg, N.; Zimmermann, H. *Mol. Cryst. Liq. Cryst.* **1985**, *126*, 225–46. Perahia, D.; Luz, Z.; Wachtel, E. J; Zimmermann, H. *Liq. Cryst.* **1987**, *2*, 473–89. Lydon, J. E. *Mol. Cryst. Liq. Cryst.* **1980**, *64*, 19–24.
(27) Attwood, T. K.; Lydon, J. E.; Jones, F. *Liq. Cryst.* **1986**, *1*, 499–507. Sadler, D. E.; Shannon, M. D.; Tollin, P.; Young, D. W.; Edmonson, M.; Rainsford, P. *Liq. Cryst.* **1986**, *1*, 509–20.
(28) Boden, N.; Bushby, R. J.; Ferris, L.; Hardy, C.; Sixl, F. *Liq. Cryst.* **1986**, *1*, 109–25.

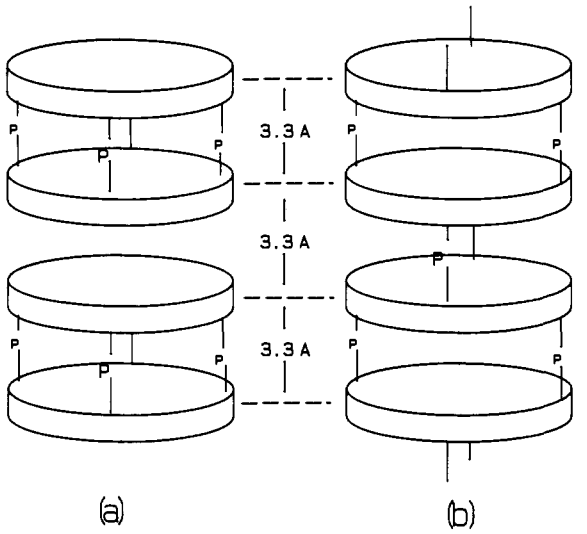

Figure 8. A sketch of two possible models for the rod structure: (a) piling of discrete pseudooctamers and (b) continuous array of cross-linked tetramers. The disks represent the guanines tetramers and P indicates the sugar-phosphodiesteric bridge. For simplicity the helical distribution along the rod axis is omitted.

without the usual segregation of polar and apolar moieties as in classical amphiphiles. In solution these molecules tend to stack in columns which may pack in a nematic or in a two-dimensional hexagonal array. Each rod is able to slide longitudinally with respect to the others.

Very elongated molecules (usually helices), such as DNA,[17,29-32] polypeptides[17,30] or polysaccharides,[14,17,30,33] can show similar phase structures: polymeric chains are aligned to give a chiral nematic order or a hexagonal array of rods.

A Plausible Model. In contrast to all other nucleic acid constituents, guanosine, guanylic acid, and some of their derivatives form gels in aqueous solutions under appropriate conditions of pH and ionic strength.[3] 5′-Guanylic acid may form other ordered structures which, however, do not aggregate into a gel.[4] The geometry of such aggregates was investigated by fiber X-ray diffraction and NMR. Although differences exist between aggregates formed by different monomers, the common feature is a helical structure formed by the stacking of tetramers in which the guanine bases interact via four hydrogen bonds[3,4] (see Figure 1): the outer hydrophylic part is formed by the sugar and, when present, by the phosphates groups. The location of the hydrophobic and hydrophylic parts is reminescent of that of DNA which also forms type II cholesteric mesophases.

In the case at hand, the magnetic behavior and the X-ray diffraction results can be explained by assuming a structure with tetrameric aromatic planes perpendicular to the rod axis and equally spaced. Since our molecular unit is a dinucleoside monophosphate, this situation can be attained in, at least, two ways.

In one case (Figure 8a) two adjacent tetrameric layers are connected by four sugar-phosphate bridges to give a pseudooctamer. The large cylindrical aggregate originates from hydrogen bonds and stacking interactions among discrete pseudooctamers. Since only one periodicity of 3.3 Å is observed, the distance between layers inside and among the pseudooctamers must be the same (within the experimental approximation).

An alternative structure (Figure 8b) can be envisaged where each layer consists of two guanosine with a free 5′-OH and two with a free 3′-OH. In such a way each tetrameric layer is covalently connected to the one above and the one below, so that the rods possess a continuous structure.

The tetrameric layers are rotated with respect to each other to form a helicoidal macrostructure. This "chiral cylinder" is the structural unit that can form either hexagonal or cholesteric mesophases depending on water content.

In our model the structural unit is rather stiff compared to the classical amphiphilic micelle. This originates from the multiplicity of attractive forces (H-bonds, stacking forces) existing inside the aggregate. The simple relationship that links the lattice constant with the concentration of d(GpG) reflects the mere dilution of the aggregate in the hexagonal array[15] and suggests that water molecules are present only outside the rods. Furthermore, the constancy of the diffraction profile with temperature confirms the ridigity of the aggregate. Also the value of the radius of the rod and the fact that it is insensitive to concentration indicate that the cross section of the aggregate is identified by a constant and discrete unit such as the guanosine tetramer whose dimension is compatible with R = 13 Å. For comparison, in the classical amphiphilic hexagonal phases the dimension of the structure elements change continuously with the water content.[20]

The presence of the peak at higher X-ray diffraction angles, corresponding to a spacing of 3.3 Å, appears to be linked to the distance between the planar tetramers of guanosines inside the columns; the presence of this peak in the cholesteric phase shows that the columns of stacked d(GpG) are already present at low concentration. The fact that the aromatic guanine bases are perpendicular to the long axis of the rod is in agreement with the negative diamagnetic anisotropy of the aggregate. In fact an alignment of the long axis of the aggregate perpendicular to the magnetic field causes the planes of guanines to lie parallel to it, and this is the preferred orientation for an aromatic molecule. The dimensions estimated by X-ray data, i.e., radius of about 13 Å and a repetition distance of 3.3 Å, were observed in some models of self-associated guanosine 5′-monophosphate. In particular using a computer molecular display and standard volumes for atomic van der Waals radii, dimensions of 12 and 3.4 Å, respectively, were obtained for the unhydrated 5′-GMP planar tetramer.[34]

Conclusions

The d(GpG)/water system exhibits two lyotropic mesophases in which the basic unit is an aggregate of d(GpG). This aggregate is rod-shaped and constituted by stacking of tetramers formed by Hoogsteen-bonded guanosines. The negative diamagnetic anisotropy and the stacking repetition of 3.3 Å in both mesophases support this model.

Also the fact that variation in concentration affects only the distance among rods and not their radius and the constancy of X-ray diffraction profile with temperature are consistent with a rather stiff aggregate whose diameter (26 Å) is compatible with the proposed model.

Acknowledgment. We thank CNR and MPI (Rome) for financial support, Professor G. Gottarelli for helpful discussions, and Dr. M. L. Capobianco for synthesis of d(GpG).

Registry No. d(GpG), 15180-30-0.

(29) Strzelecka, T. E.; Davidson, M. W.; Rill, R. L. *Nature (London)* **1988**, *331*, 457-60.
(30) Livolant, F. *J. Physique* **1986**, *47*, 1605-16.
(31) Spada, G. P.; Brigidi, P.; Gottarelli, G. *J. Chem. Soc., Chem. Commun.* **1988**, 953-4.
(32) Robinson, C. *Tetrahedron* **1961**, *13*, 219-34. Brands, R.; Kearns, D. R. *Biochemistry* **1986**, *25*, 5890-5. Skuridin, S.; Damaschun, H.; Damaschun, G.; Yevdokimov, Yu.; Misselwitz, R. *Studia Biophysica* **1986**, *112*, 139-50. Skuridin, S.; Badaev, N.; Dembo, A.; Lortkipanidze, G.; Yevdokimov, Yu. *Liq. Cryst.* **1988**, *3*, 51-62.
(33) Donald, A. M.; Viney, C.; Ritter, A. P. *Liq. Cryst.* **1986**, *1*, 287-300.
(34) Fisk, C. L.; Becker, E. D.; Miles, H. T.; Pinnavaia, T. J. *J. Am. Chem. Soc.* **1982**, *104*, 3307-14.